Antibody 10-1074 suppresses viremia in HIV-1-infected individuals

Marina Caskey[1,19], Till Schoofs[1,19], Henning Gruell[2–4,19], Allison Settler[1], Theodora Karagounis[1], Edward F Kreider[5], Ben Murrell[6], Nico Pfeifer[7], Lilian Nogueira[1], Thiago Y Oliveira[1], Gerald H Learn[5], Yehuda Z Cohen[1], Clara Lehmann[3,4], Daniel Gillor[3], Irina Shimeliovich[1], Cecilia Unson-O'Brien[1], Daniela Weiland[2–4], Alexander Robles[8], Tim Kümmerle[3], Christoph Wyen[3], Rebeka Levin[1], Maggi Witmer-Pack[1], Kemal Eren[9,10], Caroline Ignacio[6], Szilard Kiss[11], Anthony P West Jr[12], Hugo Mouquet[13], Barry S Zingman[14,15], Roy M Gulick[16], Tibor Keler[17], Pamela J Bjorkman[12], Michael S Seaman[8], Beatrice H Hahn[5], Gerd Fätkenheuer[3,4], Sarah J Schlesinger[1], Michel C Nussenzweig[1,18,19] & Florian Klein[2–4,19]

Monoclonal antibody 10-1074 targets the V3 glycan supersite on the HIV-1 envelope (Env) protein. It is among the most potent anti-HIV-1 neutralizing antibodies isolated so far. Here we report on its safety and activity in 33 individuals who received a single intravenous infusion of the antibody. 10-1074 was well tolerated and had a half-life of 24.0 d in participants without HIV-1 infection and 12.8 d in individuals with HIV-1 infection. Thirteen individuals with viremia received the highest dose of 30 mg/kg 10-1074. Eleven of these participants were 10-1074-sensitive and showed a rapid decline in viremia by a mean of 1.52 $\log_{10}$ copies/ml. Virologic analysis revealed the emergence of multiple independent 10-1074-resistant viruses in the first weeks after infusion. Emerging escape variants were generally resistant to the related V3-specific antibody PGT121, but remained sensitive to antibodies targeting nonoverlapping epitopes, such as the anti-CD4-binding-site antibodies 3BNC117 and VRC01. The results demonstrate the safety and activity of 10-1074 in humans and support the idea that antibodies targeting the V3 glycan supersite might be useful for the treatment and prevention of HIV-1 infection.

A small fraction of individuals with HIV-1 infection develop antibodies that effectively neutralize the majority of existing HIV-1 isolates[1–7]. Single-cell antibody cloning methods revealed that this serum neutralizing activity is due to one or a combination of monoclonal antibodies that target different nonoverlapping epitopes on the HIV-1 envelope spike[1,3,5,6]. These sites of vulnerability include the membrane proximal region[8–10], the base of the V3 loop and surrounding glycans[11–14], the V1/V2 loops at the apex[15,16], the CD4 binding site[17–19] and a series of epitopes that span gp120 and gp41 (refs. 20,21).

When passively transferred, many of these newly discovered antibodies protect against infection in humanized mice and macaques, even when present at very low concentrations[22–25]. In addition, combinations of antibodies targeting nonoverlapping epitopes can control active infection in humanized mice and macaques[26–29]. Finally, when they are administered in combination with agents that induce viral transcription to activate latently infected cells, antibodies decrease the incidence of viral rebound from the latent reservoir in humanized mice with HIV-1 infection[30]. These effects are in part dependent on the ability of antibodies to engage the host immune system by binding to Fc receptors expressed on a variety of host leukocytes[30–33].

These preclinical findings were extended to humans in two separate phase 1 clinical trials. A single intravenous injection of an anti-CD4-binding-site antibody—3BNC117 or VRC01—was generally safe, and it suppressed viremia by 0.8 to 2.5 $\log_{10}$ in participants infected with a virus that was sensitive to the antibody[34–36]. Moreover, 3BNC117 infusion was associated with enhanced Fc receptor-dependent clearance

of infected cells and increased breadth and potency of host anti-HIV-1 antibody responses[33,37]. Finally, in participants who carried sensitive viruses, the administration of two or four 3BNC117 30mg/kg infusions significantly delayed viral rebound during interruption of antiretroviral therapy (ART) and resulted in viral suppression for 6.7 or 9.9 weeks, respectively[38]. However, both 3BNC117 and VRC01 recognize the same target on the HIV-1 envelope protein, and whether bNAbs that target additional epitopes on the HIV-1 spike are safe and clinically effective has not been determined.

RESULTS

10-1074 shows a favorable pharmacokinetic profile and is well tolerated

10-1074 is a highly potent anti-HIV-1 antibody isolated from an individual with an HIV-1 clade A infection[11]. It targets a carbohydrate-dependent epitope in the V3 loop of the HIV-1 envelope spike[11,14]. When tested against large panels of HIV-1 pseudoviruses in TZM.bl neutralization assays *in vitro*, 10-1074 neutralizes 60.5% of 306 strains comprising 13 subtypes and 88.5% of 26 clade B strains, at an average 80% inhibitory concentration (IC_{80}) of 0.18 µg/ml and 0.13 µg/ml, respectively (**Supplementary Fig. 1a,c**)[39]. When tested against primary HIV-1 isolates from 179 individuals with HIV-1 infection (77 off and 102 on antiretroviral therapy, ART) living in the United States or in Germany, 77.7% of cultures were neutralized, with a mean IC_{80} of 0.67 µg/ml (**Supplementary Fig. 1b,c**).

To determine whether 10-1074 is safe and has antiviral activity in humans, we performed an open-label phase 1 first-in-human clinical trial. Fourteen uninfected individuals and 19 individuals with HIV-1 infection (3 on ART; 16 off ART) received a single intravenous infusion of 10-1074 at doses of 3, 10 or 30 mg/kg (**Fig. 1a**, **Table 1**, **Supplementary Fig. 2** and **Supplementary Table 1**). The antibody was generally safe and well tolerated by all participants. No grade 3, 4 or serious treatment-related adverse events or notable laboratory abnormalities were observed during a follow-up period of up to 168 d (total of 5,447 patient days; **Supplementary Table 2**).

10-1074 serum levels were determined by TZM.bl neutralization assay, which measures the amount of active antibody in the serum (**Supplementary Table 3**)[34,40–42]. Similar to 3BNC117 (refs. 34,35), 10-1074 was eliminated more rapidly in HIV-1-infected individuals
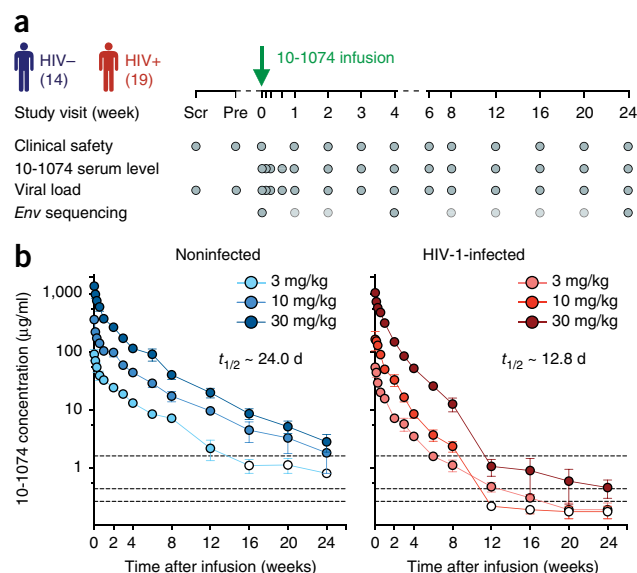

Figure 1 Study design and pharmacokinetics of 10-1074 in HIV-1-negative participants and individuals with HIV-1 infection. (**a**) Schematic representation of the study design. (**b**) Serum levels of 10-1074 as determined by TZM.bl assay. Mean values for each dose group ± s.e.m. for HIV-1-negative participants (left) and individuals with HIV-1 infection (right). Dotted horizontal lines at the bottom indicate lower limit of detection of the assays when performed using HIV-1 strains Du422.1 (top, 1.59 µg/ml), 3103.v3.c10 (middle, 0.43 µg/ml) and 3103.v3.c10 in an antiretroviral therapy-resistant backbone (bottom, 0.26 µg/ml). Each sample was measured in duplicate. Serum half-life ($t_{1/2}$) of 10-1074 between individuals with and without HIV-1 was significantly different ($P < 0.0001$). Samples demonstrating nonspecific activity were excluded from the analysis (**Supplementary Table 3**). Scr, screening visit; pre, pre-infusion visit.

than in participants without HIV-1 (**Fig. 1b**) resulting in a half-life ($t_{1/2}$) of 24.0 d and 12.8 d in individuals without and with HIV-1 infection, respectively (**Supplementary Table 4**). The differences in antibody half-life might be due to the presence of the target antigen in the individuals with HIV-1 infection and accelerated clearance of antigen–antibody immune complexes[34–36,43]. Moreover, HIV-1 infection is associated with increased levels of immunoglobulins, which potentially results in reduced antibody half-lives[44].

10-1074 reduces viremia in individuals infected with sensitive HIV-1 strains

As expected, no changes in viral load (VL) were detected after infusion in three ART-suppressed individuals (VL < 20 copies/ml) (**Table 1**, **Supplementary Tables 1** and **3a**). At the time of enrollment, HIV-1 RNA levels in the 16 individuals with HIV-1 who were not on ART ranged from 840 to 77,610 copies/ml (geometric mean of 12,851 copies/ml; **Table 1** and **Supplementary Tables 1** and **3a**). The three individuals who received a dose of 10 mg/kg of the antibody showed a rapid decrease in viremia of 1.08–1.56 $\log_{10}$ copies/ml, with a nadir at 7–9 d (**Fig. 2a**, **Supplementary Fig. 3a** and **Supplementary Table 3a**) and a return of viral RNA copy number to baseline levels within 3–4 weeks after infusion (**Fig. 2a**, **Supplementary Fig. 3a** and **Supplementary Table 3a**). Out of 13 participants with viremia who received a dose of 30 mg/kg, 11 experienced a rapid decrease in their HIV-1 RNA levels. The two individuals who failed to respond, designated 1HD2 and 1HD9K, were infected with 10-1074-resistant HIV-1 variants before undergoing 10-1074 infusion (**Fig. 2**, **Fig. 3b** and **Supplementary Fig. 4**). The average drop in viremia in individuals

Table 1 Study participant demographics.

	No HIV-1 (*n* = 14)	HIV-1 (*n* = 19)
Gender (% male)	71%	84%
Mean age (range)	43 (25–60)	39 (24–53)
Race or ethnicity		
White	36%	47%
Black or African American	43%	42%
Hispanic	7%	11%
Multiple	7%	–
Unknown	7%	–
ART status at enrollment		
On ART n (%)	–	3 (16%)
Off ART n (%)	–	16 (84%)
CD4+ T cell count (day 0)		
Mean absolute (cells/µl)	–	593 (289–880)
Mean relative (%)	–	30% (11–49%)
HIV-1 RNA levels (day 0)*		
Geometric mean (copies/ml)	–	12,851 (840–77,610)
Mean log	–	4.11 (2.92–4.89)

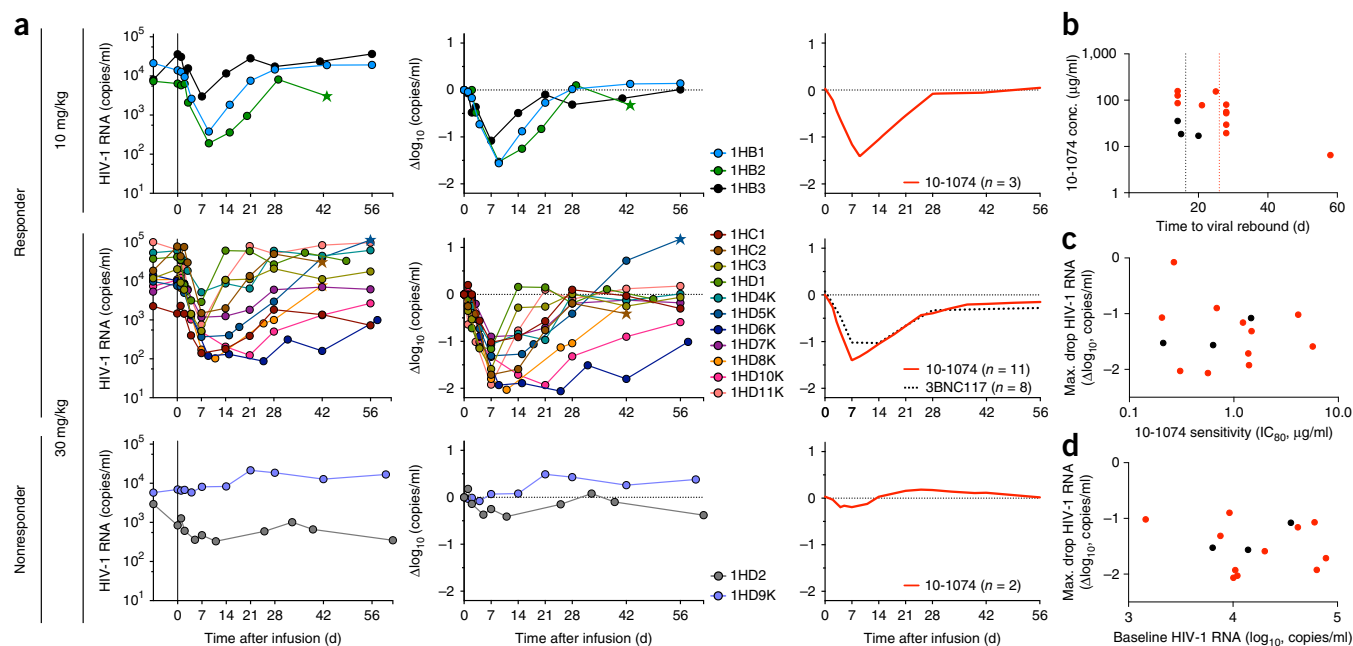Asterisk (*), HIV-1 RNA levels in individuals off ART on day 0.

Figure 2 Viral load dynamics after 10-1074 infusion in participants with HIV-1. (**a**) 10-1074 dose of either 10 or 30 mg/kg is indicated on the left. Left graphs show absolute viral loads in HIV-1 RNA copies/ml (*y* axis) versus time in days after infusion (*x* axis). Middle graphs demonstrate $\log_{10}$ changes in HIV-1 RNA levels from day 0. Right graphs show average $\log_{10}$ change in viremia after 10-1074 (red line) or 3BNC117 infusion[34] (dotted black; curves were fitted by robust lowess regression with 40% of the data using MATLAB_R2016a). At the 30-mg/kg dose level, viremia was significantly suppressed from about day 3 to day 27 post-infusion as compared to viral load at day 0. The window of significant viral suppression was assessed by computing simultaneous confidence bands and determined when these excluded zero (**Supplementary Fig. 5**). Stars indicate the initiation of antiretroviral therapy. (**b**) 10-1074 serum levels at the time of rebound for individuals receiving 10 or 30 mg/kg of 10-1074 (black or red circles, respectively). Dotted lines indicate mean time to rebound after 10-1074 infusion (black, 10 mg/kg, and red, 30 mg/kg). (**c**) Maximum $\log_{10}$ decline in viremia as measured by RNA copies/ml versus 10-1074 IC_{80} (Spearman coefficient rho = −0.05; *P* = 0.88) of primary culture virus from samples obtained 557 d to 61 d before infusion as determined by TZM.bl assay. No sensitivity data were obtained from 1HC2, 1HD2 and 1HD10K before enrollment. Colors as in **b**. (**d**) Maximum $\log_{10}$ decline in viremia in 10-1074-sensitive individuals versus initial viral load as measured by RNA copies/ml (Spearman coefficient rho = −0.19; *P* = 0.52). Colors as in **b**.

who received 30 mg/kg of 10-1074 and harbored sensitive strains was 1.52 $\log_{10}$ copies/ml (range, 0.9–2.06 $\log_{10}$ copies/ml). The nadir was reached after an average of 10.3 d (range 7–25 d). When compared to pretreatment HIV-1 RNA levels (day 0), the decrease in viremia in this group was significant from about day 3 to day 27 post-infusion (**Fig. 2a**, **Supplementary Table 3a** and **Supplementary Fig. 5**). The average 10-1074 serum concentrations at viral rebound (defined as an increase of at least 0.5 $\log_{10}$ copies/ml above nadir and confirmed in the follow-up visit) were 23.7 and 76.9 µg/ml in the 10 and 30 mg/kg dose groups, respectively (**Fig. 2b**). The most sustained response, 58 d, occurred in individual 1HD6K, who exhibited a 10-1074 concentration of 6.5 µg/ml at rebound (**Fig. 2b**). Maximum drop in viral load, ($\Delta \log_{10}$ copies/ml) was not correlated with the 10-1074 neutralization sensitivity (IC_{80}) of primary virus cultures obtained before infusion (Spearman's rho: −0.05) or with baseline viremia (Spearman's rho = −0.19) (**Fig. 2c,d**). Relative T cell subsets remained unchanged (**Supplementary Fig. 6** and **Supplementary Table 3a**). We conclude that 10-1074 administration rapidly decreases viremia in individuals infected with sensitive HIV-1 strains.

Viremia at rebound contains a mixture of different escape variants
To examine the precise nature of the virologic effects of 10-1074 infusion, we performed single-genome sequencing (SGS) before and after infusion on circulating viruses from 15 out of 16 individuals with viremia. We retrieved a total of 1,111 full-length envelope sequences (**Supplementary Table 5**). Study subjects were infected with

epidemiologically distinct clade B viruses (**Fig. 3a** and **Supplementary Fig. 4**). Consistently with different durations of HIV-1 infection, day 0 *env* diversity and phylogenetic complexity varied between participants (**Fig. 3a** and **Supplementary Fig. 4**).

The 10-1074 antibody makes crucial contacts with Env glycans at a potential *N*-linked glycosylation site (PNGS) at position N332 and with the ^{324}G(D/N)IR^{327} motif at the base of the V3 loop[11,14,45]. With the exception of the two individuals who were resistant to 10-1074 (1HD2 and 1HD9K) and participant 1HC1, all day-0 plasma *env* sequences in the remaining ten individuals displayed a PNGS at position N332 and an intact ^{324}G(D/N)IR^{327} motif, which suggests that the corresponding viruses are sensitive to 10-1074 (**Fig. 3b**, **Supplementary Fig. 4** and **Supplementary Table 5**). Individual 1HC1, who responded to 10-1074 infusion with a drop of only 1.0 $\log_{10}$ copies/ml in viremia, carried an N332T mutation in 2 of 19 viruses sequenced before infusion (**Fig. 3b** and **Supplementary Fig. 4**). The two individuals who did not respond carried single amino acid (AA) mutations at either the PNGS (N332T in 1HD2) or a 10-1074 contact residue in the protein-binding motif (D325E in 1HD9K) in 100% of day-0 plasma *env* sequences (**Fig. 3b** and **Supplementary Fig. 4**).

Four weeks after infusion, 370 intact envelope sequences were obtained from 13 individuals who responded to 10-1074. Over 91% of sequences showed recurrent AA mutations, most of which (97%) eliminated the PNGS at position 332 by mutating either N332 or S334 (**Fig. 3c,d**). 3% of mutated sequences showed changes at D/N325 in
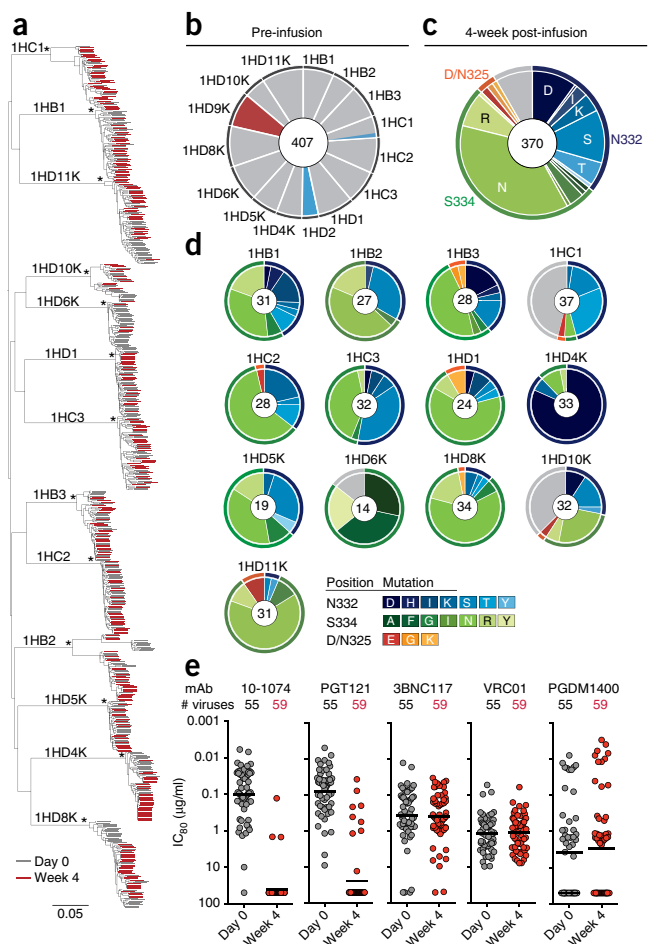
Figure 3 Viral evolution after 10-1074 infusion in participants with HIV-1 infection. (**a**) Maximum-likelihood phylogenetic tree of single-genome-derived *env* gene sequences obtained from plasma before (day 0, gray) and 4 weeks after 10-1074 infusion (week 4, red). Asterisks indicate nodes with bootstrap support of 100% (100 replicates). (**b**) Frequency of resistance mutations found in circulating viruses by SGS before infusion for each individual. Gray indicates the absence of potential resistance mutation at positions 325, 332 and 334. Colors correspond to mutations indicated in **c**. For all pie charts, the number of analyzed sequences is shown in the center. (**c**) Amino acid frequencies at three recurrently mutated 10-1074 contact sites for all pooled circulating virus sequences obtained by SGS 4 weeks after infusion. Outer rings indicate position of mutation (orange, 325; blue, 332; green, 334; gray, not mutated). (**d**) As in **c**, but for each individual. Colors indicate the type of mutation. For 1HD6K and 1HD10K, both week 4 and week 8 were included in **c** and **d**. (**e**) Sensitivity to the indicated anti-HIV-1 antibodies of 114 different viral isolates obtained from 11 individuals before (gray, 55 isolates) and 4 weeks after 10-1074 infusion (red, 59 isolates) with IC_{80} values (µg/ml) on the y axis (log_{10} scale). Each dot represents one viral isolate. Lines indicate geometric mean. Samples were run in duplicate.
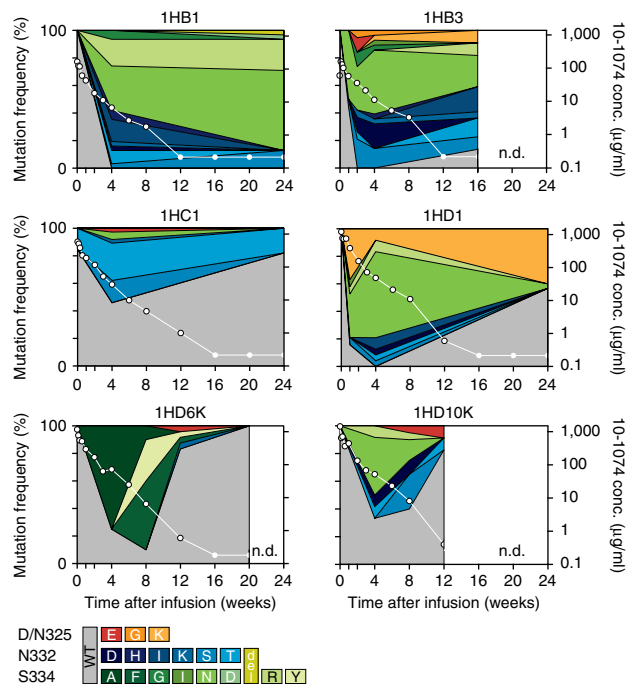

Figure 4 Temporal evolution of escape from 10-1074 over time in individuals 1HB1, 1HB3, 1HC1, 1HD1, 1HD6K and 1HD10K. Plots display relative frequencies of escape mutations observed in SGS data at envelope positions 325, 332 and 334 as shaded areas over time. Sequencing was performed on day 0 (all subjects) and at week 1 (1HB3, 1HD1), week 2 (1HB3), week 4 (all subjects), week 8 (1HD6K, 1HD10K), week 12 (1HD6K, 1HD10K), week 16 (1HB3), week 20 (1HD6K) and week 24 (1HB1, 1HC1, 1HD1) (see **Supplementary Table 5** for absolute numbers). White line indicates serum concentration of 10-1074 as determined by TZM.bl assay (**Supplementary Table 3**). White circles without border depict 10-1074 serum levels below the limit of detection.

the ^{324}G(D/N)IR^{327} motif (**Fig. 3c,d** and **Supplementary Table 5**). Viral sequences comprised a mixture of different variants, all of which were closely related to pre-infusion day-0 viruses, which highlights the multiclonal origin of rebound viremia (**Fig. 3a** and **Supplementary Fig. 4**). Mutations at AA positions 325, 332 and 334 were mutually exclusive with mutations at only one of three positions in any given virus (**Supplementary Fig. 4**). Two of the most frequent mutations, S334N and N332S, were found in 12/13 (S334N) and 11/13 (N332S) of the individuals analyzed (**Fig. 3c,d** and **Supplementary Fig. 4**).

On the nucleotide level, 99% (319 out of 322) of mutations affecting the PNGS at N332 were due to a single change relative to day 0 (**Supplementary Fig. 7**). The majority of these mutations were transitions, consistent with reverse transcriptase (RT) errors[46]. Day-0 viruses from 10 out of 13 individuals who responded to 10-1074 infusion carried the triplets AAC-ATT-AGT at positions 332–334 in 99% of their pre-infusion sequences (**Supplementary Fig. 7**). Notably, these individuals exhibited a very similar spectrum of AA escape mutations at week 4 (**Fig. 3d** and **Supplementary Fig. 7**). By contrast, individual 1HD6K, who maintained viral suppression for over 8 weeks, exhibited a different set of codons, i.e., AAT-ATT-TCT, in the antibody target region. This probably resulted in a different spectrum of escape mutations, which indicates that the codon composition in this region might influence viral escape from 10-1074 (**Fig. 3d** and **Supplementary Fig. 7**).

To determine whether loss of the PNGS at position N332 or ^{324}G(D/N)IR^{327} mutation is associated with resistance to 10-1074, we performed neutralization assays on 114 pseudoviruses expressing envelope proteins derived from circulating viruses on day 0 (55 pseudoviruses) and 4 weeks (59 pseudoviruses) after 10-1074 infusion (**Fig. 3e**, **Supplementary Fig. 4** and **Supplementary Table 6**). The pseudoviruses were tested against antibodies currently in, or being considered for, clinical testing. These include 3BNC117 and VRC01, which target the CD4 binding site[34–36,38]; 10-1074 and PGT121, which recognize the base of the V3 loop and surrounding glycans[11,12]; and PGDM1400, which recognizes a conformational epitope at the top of
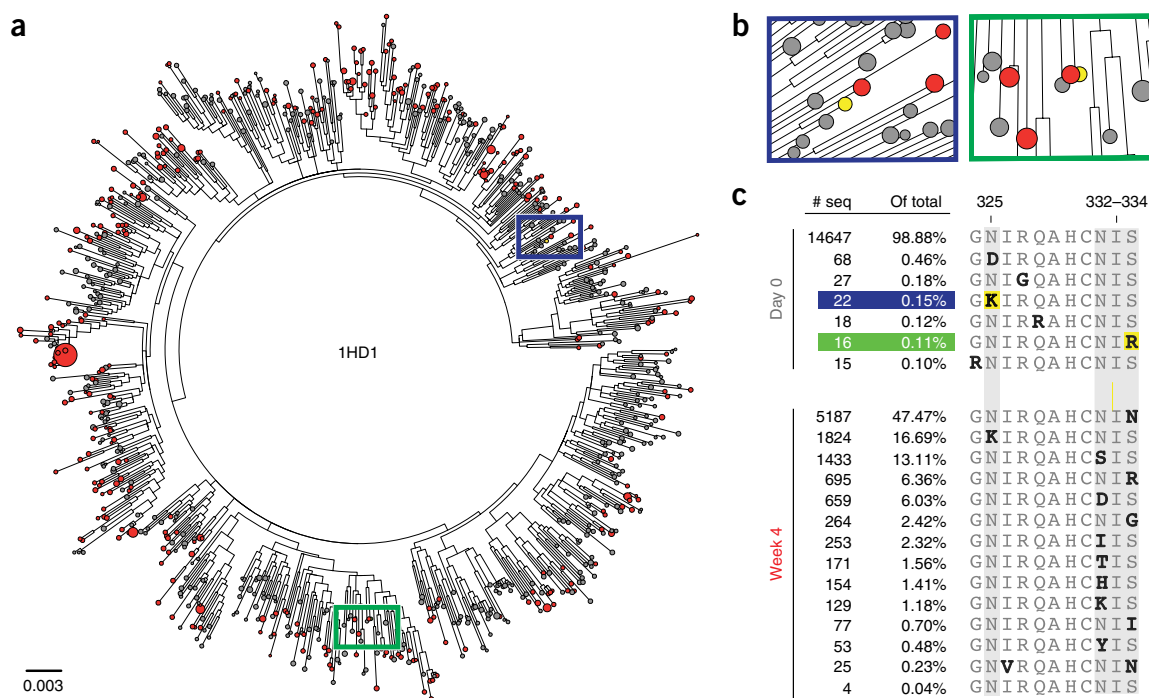
Figure 5 SMRT sequencing analysis. (**a**) Maximum-likelihood phylogenetic tree of full-length plasma envelope sequences obtained on day 0 and week 4 after 10-1074 infusion from individual 1HD1. Branches show high-quality consensus sequences (HQCSs) with their respective copy number visualized as the size of the colored circle (day 0, gray; week 4, red). (**b**) Insets highlight two day-0 minority variants that carry 10-1074 escape mutations ^{324}GKIR^{327} (blue, mutation in yellow) and ^{332}NIR^{334} (green, mutation in yellow). (**c**) Number of filtered reads for the indicated sequence variants at positions 324–334 and the relative frequency of each variant. Residues 325 and 332–334 are shaded in gray. Deviations from the day-0 majority variant are in bold.

the envelope spike[16]. PGT121 differs from 10-1074 in that it interacts more strongly with glycans at positions N137, N156 and N301, and as a result, PGT121 is thought to be less dependent on the glycan at N332 than 10-1074 (refs. 13,14).

As expected, there was no correlation between the emergence of resistance to 10-1074 and resistance to antibodies targeting non-overlapping sites on the HIV-1 Env protein (3BNC117, VRC01 or PGDM1400; **Fig. 3e**). Consistent with data obtained by examining large panels of HIV-1 pseudoviruses, there was no significant difference in sensitivity against 10-1074 and PGT121 (mean$_{GEO}$ IC$_{80}$ = 0.10 versus 0.08 µg/ml; P = 0.19; **Fig. 3e**) and 3BNC117 was generally more potent than VRC01 (mean$_{GEO}$ IC$_{80}$ = 0.37 versus 1.18 µg/ml; P = 5.1 × 10^{-6}; **Fig. 3e**). In 10 of 11 individuals from whom envelopes were tested, HIV-1 strains that developed resistance to 10-1074 were also resistant to PGT121 (**Supplementary Table 6**). Thus, the interaction between PGT121 and additional glycans on the Env protein had little impact on the neutralizing potency of PGT121 on the naturally arising N332 or ^{324}G(D/N)IR^{327} viral variants tested.

We also analyzed the composition of observed escape mutations in HIV-1 variants in six individuals over time. In all six individuals, the relative abundance of escape variants changed (**Fig. 4**). In addition, in five of six individuals, strains carrying the intact ^{324}G(D/N)IR^{327} protein motif and a PNGS at N332 re-emerged at 12, 16 or 24 weeks after infusion at a time when 10-1074 levels approached or were below the limit of detection (**Fig. 4**). This indicates ongoing selection for both resistance and/or viral fitness after 10-1074 infusion.

Escape variants are pre-existing or rapidly generated
Previous studies suggest that high viral turnover in HIV-1 infection results in a multitude of circulating mutant strains in any given

individual[47,48]. To examine the dynamics of early viral escape, we sequenced viruses present in the plasma 1 week after 10-1074 administration in seven individuals (**Supplementary Fig. 8** and **Supplementary Table 5**). We found a mixture of nonmutated and N332-PNGS- or ^{324}G(D/N)IR^{327}-mutant viruses. Moreover, the frequency of escape variants at this early time point after infusion was inversely correlated with the duration of viral suppression (R^2 = 0.73) (**Supplementary Fig. 8**).

The kinetics of escape are consistent with pre-existing resistant viral variants in circulation at the time of infusion and/or rapid *de novo* generation of these mutations. To estimate the frequency of pre-existing variants and to assess how they contribute to 10-1074 escape, we performed primer-ID-based deep sequencing (PIDS) of the V3-loop region[49,50] on plasma samples from five study participants. A total of 2,077 and 1,844 viral consensus sequences were obtained at day 0 and week 4, respectively (**Supplementary Table 7**). The obtained sampling depth was powered to detect a mutation present in 1.0% (range, 0.5–2.4%) of the viral population with 95% confidence. Whereas mutations at positions 325, 332 or 334 were found in 99.8% of the sequences in the week 4 samples, none were observed at day 0 (**Supplementary Table 7**). This indicates that the rate of potential pre-existing escape mutations is probably lower than 1.0%.

We also performed full-length envelope deep sequencing (single-molecule real-time (SMRT) sequencing) of day 0 and week 4 samples from three of the same individuals (**Fig. 5** and **Supplementary Table 8**)[51]. Frequencies of detected variants carrying a 325 or 332–334 mutation agreed well among SMRT sequencing, PIDS and SGS (**Supplementary Table 8**). A phylogenetic tree of SMRT sequences confirmed that escape variants arose from multiple independent HIV-1 viruses (**Fig. 5** and **Supplementary Fig. 9**). Out of a total of

30,711 day-0 sequences obtained by SMRT sequencing, we found D/N325K and S334R mutations in individual 1HD1 at a rate of 0.15% and 0.11%, respectively, and the S334N mutation at a rate of 0.34% in individual 1HB3. No 325 or 332–334 mutants were detected in individual 1HC2 (**Fig. 5** and **Supplementary Fig. 9**). We conclude that circulating pre-existing variants carrying mutations at key positions associated with resistance to 10-1074 can be detected at very low frequency in individuals who are considered sensitive to the antibody, and that resistance originates from multiple viral variants.

DISCUSSION

Antibodies have a unique role in the therapeutic armamentarium against human cancers and inflammatory diseases because they engage the host immune system to attack tumor cells or modify inflammatory responses by binding to Fc receptors on host leukocytes. Similarly, in individuals with HIV-1 infection, passively transferred antibodies accelerate the clearance of infected cells and induce host immunity against HIV-1 (refs. 30,32,33,37). These unique features of immunotherapy suggest that antibodies should be further explored as adjuncts to conventional ART for the prevention or treatment of HIV-1 infection.

Anti-CD4-binding-site antibodies 3BNC117 and VRC01 have been generally safe and effective at decreasing plasma HIV-1 RNA levels[34,35] and preventing rebound viremia during analytical treatment interruption in humans[38,52]. The two antibodies differ in their relative potency and half-lives; 3BNC117 has a somewhat longer half-life and greater potency than VRC01 (refs. 34,35,38). As expected, these properties are reflected by the relative ability of the two antibodies to prevent infection in macaques and to prolong viral suppression in humans undergoing analytical treatment interruption[38,52]. The finding that 10-1074 has favorable safety and pharmacokinetics profiles and is effective at decreasing viremia extends these observations to an additional nonoverlapping target of vulnerability on the HIV-1 spike.

10-1074 is more potent and has a comparable half-life to, but has a narrower spectrum of activity than, either of the two CD4-binding-site antibodies. Its effect on viremia is similar to 3BNC117, but a higher frequency of fully resistant escape variants was detected for 10-1074 than for 3BNC117 (refs. 34,37,38). We speculate that this difference in occurrence of escape might be due to the relative cost of altering the CD4 binding site, which makes viable escape from antibodies that target this site more difficult, as has been shown *in vitro*[53]. As a consequence, the number of distinct escape variants that can give rise to high-level viremia might be reduced. This idea is consistent with the relative paucity of naturally arising viruses that are resistant to 3BNC117 in comparison to 10-1074 or all other glycan patch bNAbs[54]. However, we did observe that 10-1074 escape mutations are selected against in several individuals when antibody levels drop. This finding suggests that these mutations are also associated with a fitness cost *in vivo*.

In humanized mice and in humans, a single antibody, such as a single small-molecule drug, is insufficient to prevent the emergence of resistant viral variants because the infection produces a swarm of related mutant viruses[26,34,35,55]. Similarly to what has been described for small-molecule drugs, resistance to antibodies seems to arise from pre-existing minority variants and/or *de novo* mutations produced during rapid HIV-1 turnover. Our findings underscore some of the similarities in antiviral activity between small-molecule drugs and antibodies and emphasize that combinations of antibodies that target nonoverlapping epitopes will be required for effective therapy and possibly prevention.

10-1074 targets an epitope that is distinct from other second-generation bNabs that have been tested in humans[34,35]. It has favorable clinical characteristics and potent anti-viral activity, and therefore, 10-1074 is a promising candidate for antibody-mediated combination immunotherapy and the prevention of HIV-1 infection.

METHODS

Methods, including statements of data availability and any associated accession codes and references, are available in the online version of the paper.

Note: Any Supplementary Information and Source Data files are available in the online version of the paper.

COMPETING FINANCIAL INTERESTS STATEMENT

The authors declare competing financial interests: details are available in the online version of the paper.

Reprints and permissions information is available online at http://www.nature.com/reprints/index.html.

1. Klein, F. *et al.* Antibodies in HIV-1 vaccine development and therapy. *Science* **341**, 1199–1204 (2013).
2. Hraber, P. *et al.* Prevalence of broadly neutralizing antibody responses during chronic HIV-1 infection. *AIDS* **28**, 163–169 (2014).
3. West, A.P. Jr. *et al.* Structural insights on the role of antibodies in HIV-1 vaccine and therapy. *Cell* **156**, 633–648 (2014).
4. Mikell, I. *et al.* Characteristics of the earliest cross-neutralizing antibody response to HIV-1. *PLoS Pathog.* **7**, e1001251 (2011).
5. Burton, D.R. & Mascola, J.R. Antibody responses to envelope glycoproteins in HIV-1 infection. *Nat. Immunol.* **16**, 571–576 (2015).
6. Haynes, B.F. *et al.* HIV-host interactions: implications for vaccine design. *Cell Host Microbe* **19**, 292–303 (2016).
7. Moore, P.L., Williamson, C. & Morris, L. Virological features associated with the development of broadly neutralizing antibodies to HIV-1. *Trends Microbiol.* **23**, 204–211 (2015).
8. Buchacher, A. *et al.* Generation of human monoclonal antibodies against HIV-1 proteins; electrofusion and Epstein-Barr virus transformation for peripheral blood lymphocyte immortalization. *AIDS Res. Hum. Retroviruses* **10**, 359–369 (1994).
9. Muster, T. *et al.* A conserved neutralizing epitope on gp41 of human immunodeficiency virus type 1. *J. Virol.* **67**, 6642–6647 (1993).
10. Huang, J. *et al.* Broad and potent neutralization of HIV-1 by a gp41-specific human antibody. *Nature* **491**, 406–412 (2012).
11. Mouquet, H. *et al.* Complex-type N-glycan recognition by potent broadly neutralizing HIV antibodies. *Proc. Natl. Acad. Sci. USA* **109**, E3268–E3277 (2012).
12. Walker, L.M. *et al.* Broad neutralization coverage of HIV by multiple highly potent antibodies. *Nature* **477**, 466–470 (2011).
13. Sok, D. *et al.* Promiscuous glycan site recognition by antibodies to the high-mannose patch of gp120 broadens neutralization of HIV. *Sci. Transl. Med.* **6**, 236ra63 (2014).
14. Garces, F. *et al.* Structural evolution of glycan recognition by a family of potent HIV antibodies. *Cell* **159**, 69–79 (2014).
15. Walker, L.M. *et al.* Broad and potent neutralizing antibodies from an African donor reveal a new HIV-1 vaccine target. *Science* **326**, 285–289 (2009).
16. Sok, D. *et al.* Recombinant HIV envelope trimer selects for quaternary-dependent antibodies targeting the trimer apex. *Proc. Natl. Acad. Sci. USA* **111**, 17624–17629 (2014).
17. Scheid, J.F. *et al.* Sequence and structural convergence of broad and potent HIV antibodies that mimic CD4 binding. *Science* **333**, 1633–1637 (2011).
18. Wu, X. *et al.* Rational design of envelope identifies broadly neutralizing human monoclonal antibodies to HIV-1. *Science* **329**, 856–861 (2010).
19. Liao, H.X. *et al.* Co-evolution of a broadly neutralizing HIV-1 antibody and founder virus. *Nature* **496**, 469–476 (2013).
20. Scharf, L. *et al.* Antibody 8ANC195 reveals a site of broad vulnerability on the HIV-1 envelope spike. *Cell Rep.* **7**, 785–795 (2014).
21. Huang, J. *et al.* Broad and potent HIV-1 neutralization by a human antibody that binds the gp41-gp120 interface. *Nature* **515**, 138–142 (2014).
22. Pietzsch, J. *et al.* A mouse model for HIV-1 entry. *Proc. Natl. Acad. Sci. USA* **109**, 15859–15864 (2012).
23. Moldt, B. *et al.* Highly potent HIV-specific antibody neutralization in vitro translates into effective protection against mucosal SHIV challenge *in vivo. Proc. Natl. Acad. Sci. USA* **109**, 18921–18925 (2012).
24. Gautam, R. *et al.* A single injection of anti-HIV-1 antibodies protects against repeated SHIV challenges. *Nature* **533**, 105–109 (2016).
25. Shingai, M. *et al.* Passive transfer of modest titers of potent and broadly neutralizing anti-HIV monoclonal antibodies block SHIV infection in macaques. *J. Exp. Med.* **211**, 2061–2074 (2014).
26. Klein, F. *et al.* HIV therapy by a combination of broadly neutralizing antibodies in humanized mice. *Nature* **492**, 118–122 (2012).
27. Horwitz, J.A. *et al.* HIV-1 suppression and durable control by combining single broadly neutralizing antibodies and antiretroviral drugs in humanized mice. *Proc. Natl. Acad. Sci. USA* **110**, 16538–16543 (2013).
28. Barouch, D.H. *et al.* Therapeutic efficacy of potent neutralizing HIV-1-specific monoclonal antibodies in SHIV-infected rhesus monkeys. *Nature* **503**, 224–228 (2013).
29. Shingai, M. *et al.* Antibody-mediated immunotherapy of macaques chronically infected with SHIV suppresses viraemia. *Nature* **503**, 277–280 (2013).
30. Halper-Stromberg, A. *et al.* Broadly neutralizing antibodies and viral inducers decrease rebound from HIV-1 latent reservoirs in humanized mice. *Cell* **158**, 989–999 (2014).
31. Hessell, A.J. *et al.* Fc receptor but not complement binding is important in antibody protection against HIV. *Nature* **449**, 101–104 (2007).
32. Bournazos, S. *et al.* Broadly neutralizing anti-HIV-1 antibodies require Fc effector functions for in vivo activity. *Cell* **158**, 1243–1253 (2014).
33. Lu, C.L. *et al.* Enhanced clearance of HIV-1-infected cells by broadly neutralizing antibodies against HIV-1 in vivo. *Science* **352**, 1001–1004 (2016).
34. Caskey, M. *et al.* Viraemia suppressed in HIV-1-infected humans by broadly neutralizing antibody 3BNC117. *Nature* **522**, 487–491 (2015).
35. Lynch, R.M. *et al.* Virologic effects of broadly neutralizing antibody VRC01 administration during chronic HIV-1 infection. *Sci. Transl. Med.* **7**, 319ra206 (2015).
36. Ledgerwood, J.E. *et al.* Safety, pharmacokinetics and neutralization of the broadly neutralizing HIV-1 human monoclonal antibody VRC01 in healthy adults. *Clin. Exp. Immunol.* **182**, 289–301 (2015).
37. Schoofs, T. *et al.* HIV-1 therapy with monoclonal antibody 3BNC117 elicits host immune responses against HIV-1. *Science* **352**, 997–1001 (2016).
38. Scheid, J.F. *et al.* HIV-1 antibody 3BNC117 suppresses viral rebound in humans during treatment interruption. *Nature* **535**, 556–560 (2016).
39. Yoon, H. *et al.* CATNAP: a tool to compile, analyze and tally neutralizing antibody panels. *Nucleic Acids Res.* **43**, W213–W219 (2015).
40. Li, M. *et al.* Human immunodeficiency virus type 1 env clones from acute and early subtype B infections for standardized assessments of vaccine-elicited neutralizing antibodies. *J. Virol.* **79**, 10108–10125 (2005).
41. Seaman, M.S. *et al.* Tiered categorization of a diverse panel of HIV-1 Env pseudoviruses for assessment of neutralizing antibodies. *J. Virol.* **84**, 1439–1452 (2010).
42. Sarzotti-Kelsoe, M. *et al.* Optimization and validation of the TZM-bl assay for standardized assessments of neutralizing antibodies against HIV-1. *J. Immunol. Methods* **409**, 131–146 (2014).
43. Keizer, R.J., Huitema, A.D., Schellens, J.H. & Beijnen, J.H. Clinical pharmacokinetics of therapeutic monoclonal antibodies. *Clin. Pharmacokinet.* **49**, 493–507 (2010).
44. Moir, S. & Fauci, A.S. B cells in HIV infection and disease. *Nat. Rev. Immunol.* **9**, 235–245 (2009).
45. Gristick, H.B. *et al.* Natively glycosylated HIV-1 Env structure reveals new mode for antibody recognition of the CD4-binding site. *Nat. Struct. Mol. Biol.* **23**, 906–915 (2016).
46. Abram, M.E., Ferris, A.L., Shao, W., Alvord, W.G. & Hughes, S.H. Nature, position, and frequency of mutations made in a single cycle of HIV-1 replication. *J. Virol.* **84**, 9864–9878 (2010).
47. Coffin, J.M. HIV population dynamics in vivo: implications for genetic variation, pathogenesis, and therapy. *Science* **267**, 483–489 (1995).
48. Maldarelli, F. *et al.* HIV populations are large and accumulate high genetic diversity in a nonlinear fashion. *J. Virol.* **87**, 10313–10323 (2013).
49. Zhou, S., Jones, C., Mieczkowski, P. & Swanstrom, R. Primer ID validates template sampling depth and greatly reduces the error rate of next-generation sequencing of HIV-1 genomic RNA populations. *J. Virol.* **89**, 8540–8555 (2015).
50. Bhiman, J.N. *et al.* Viral variants that initiate and drive maturation of V1V2-directed HIV-1 broadly neutralizing antibodies. *Nat. Med.* **21**, 1332–1336 (2015).
51. Laird Smith, M. *et al.* Rapid Sequencing of Complete env Genes from Primary HIV-1 Samples. in *Virus Evolution* (Oxford University Press, 2016).
52. Bar, K.J. *et al.* Effect of HIV Antibody VRC01 on Viral Rebound after Treatment Interruption. *N. Engl. J. Med.* **375**, 2037–2050 (2016).
53. Lynch, R.M. *et al.* HIV-1 fitness cost associated with escape from the VRC01 class of CD4 binding site neutralizing antibodies. *J. Virol.* **89**, 4201–4213 (2015).
54. West, A.P. Jr. *et al.* Computational analysis of anti-HIV-1 antibody neutralization panel data to identify potential functional epitope residues. *Proc. Natl. Acad. Sci. USA* **110**, 10598–10603 (2013).
55. Trkola, A. *et al.* Delay of HIV-1 rebound after cessation of antiretroviral therapy through passive transfer of human neutralizing antibodies. *Nat. Med.* **11**, 615–622 (2005).

ONLINE METHODS

10-1074 study drug. 10-1074 is a recombinant, fully human IgG1λ mAb recognizing the base of the V3 loop and surrounding glycans on the HIV-1 envelope[11]. 10-1074 was cloned from an African donor (patient 10)[56] infected with an HIV-1 clade A virus[11]. It was expressed in Chinese hamster ovary cells (clone 3G4) and purified by using standard methods. The 10-1074 drug substance was produced at Celldex Therapeutics' Fall River (Massachusetts) GMP facility, and the drug product was fill-finished at Althea Technologies (California). The resulting purified 10-1074 was supplied as a single-use sterile 20 mg/ml solution for intravenous injection in a 5.0-ml volume of buffered solution composed of sodium phosphate, potassium phosphate, potassium chloride, sodium chloride and polysorbate 80 with a pH of 7.0. 10-1074 vials were shipped and stored at 4 °C.

Study design. An open-label, dose-escalation phase 1 study (ClinicalTrials.gov: NCT02511990, EudraCT: 2015-004574-15) was conducted in individuals with HIV-1 (group 1) and without HIV-1 (group 2) to evaluate the safety, pharmacokinetics and antiviral activity of 10-1074. Study participants were enrolled sequentially according to eligibility criteria. A standard "3 + 3" phase 1 trial design was used in the dose-escalation phase of the study. 10-1074 was administered as a single intravenous infusion over 60 min at three dose levels: 3 mg/kg (subjects 1HA1-1HA3, 2HA1-2HA3), 10 mg/kg (subjects 1HB1-1HB3, 2HB1-2HB3) or 30 mg/kg (subjects 1HC1- 1HC3, 1HD1, 1HD2, 1HD4K-1HD11K, 2HC1-2HC3, 2HD1-2HD5). Study participants were followed for 84–168 d (24 weeks) after infusion. All participants provided written informed consent before participation in the study, and the study was conducted in accordance with Good Clinical Practice. The protocol was approved by the Federal Drug Administration in the USA, the Paul Ehrlich Institut in Germany and the Institutional Review Boards (IRBs) at the Rockefeller University and the University of Cologne. All trial-related measures for subjects recruited at Montefiore were conducted at Rockefeller University Hospital (including informed consent and screening procedures).

Study participants. All study participants were recruited at the Rockefeller University Hospital, New York, USA, at the University Hospital Cologne, Cologne, Germany, or at Montefiore Medical Center, New York, USA. Eligible subjects were adults aged 18–65 years, either with or without HIV-1 and without concomitant hepatitis B or C infections. Individuals with HIV-1 enrolled in study group 1A were on ART with plasma HIV-1 RNA levels <20 copies/ml, and they received a single 3 mg/kg 10-1074 infusion. In groups 1B through 1D, subjects were off ART (ART-experienced or ART-naïve) for at least 8 weeks before participation in the study and had plasma HIV-1 RNA levels <100,000 copies/ml, measured on two separate occasions at least 1 week apart, and received a single 10 mg/kg (1B) or 30 mg/kg (1C-1D) 10-1074 infusion. Baseline sensitivity of viruses from outgrowth cultures to 10-1074 was known for all subjects enrolled in groups 1A–D, with the exception of 1HC2, 1HD2 and 1HD10K. Individuals with CD4+ T cell counts <300 cells/μl, clinically relevant deviations from normal physical findings and/or laboratory examinations were excluded. Screening period was from day −49 to day −7 before infusion, and the window for the pre-infusion visit was from day −42 to day −1 before infusion. Race was recorded as self-reported. Women of childbearing age were required to have a negative serum pregnancy test on the day of 10-1074 infusion. Individuals with HIV-1 who were not on ART at enrollment were encouraged to initiate ART 6 weeks after 10-1074 infusion.

Study procedures. The appropriate volume of 10-1074 was calculated according to study dose group, diluted in sterile normal saline to a total volume of 100 or 250 ml and administered intravenously over 60 min. Study participants received 10-1074 on day 0 and remained under close monitoring in the infusion unit of the Rockefeller University Hospital or the University Hospital Cologne for 24 h. Participants returned for frequent follow-up visits for safety assessments that included physical examination and measurement of clinical laboratory parameters, such as hematology, chemistries, urinalysis, coagulation times and pregnancy tests, as well as HIV-1 viral load and CD4+ and CD8+ T cell counts (**Fig. 1a**). Adverse events were graded according to the DAIDS Table for Grading the Severity of Adult and Pediatric Adverse Events (version 2.0, November 2014) (groups with HIV-1) or the Toxicity Grading Scale for Healthy Adult and Adolescent Volunteers Enrolled in Preventive Vaccine Clinical Trials (September 2007) (uninfected groups). Blood samples (30–120 ml) were collected before and at multiple times after 10-1074 infusion. Samples were processed within 4 h of collection, and serum and plasma samples were stored at −80 °C. Peripheral blood mononuclear cells (PBMCs) were isolated by density gradient centrifugation. The absolute number of PBMCs was determined by an automated cell counter (Vi-Cell XR; Beckman Coulter) or manually, and cells were cryopreserved in FBS plus 10% DMSO.

Plasma HIV-1 RNA levels. Plasma was collected for measuring HIV-1 RNA levels at screening (from day −49 to day −7), the pre-infusion visit (from day −42 to day −1), day 0 (before infusion) and on days 1, 2, 4, 7, 14, 21, 28, 42, 56, 84, 112, 140 and 168. HIV-1 RNA levels were determined using the Roche COBAS AmpliPrep/COBAS TaqMan HIV-1 Assay, Version 2.0 or the Roche Cobas 6800 HIV-1 kit, which detect from 20 copies/ml to 10×10^6 copies/ml.

CD4+ and CD8+ T cells. CD4+ and CD8+ T cell counts were determined at screening, on day 0 (before infusion), days 7, 14, 28, 56, 112 and 168 by a clinical flow cytometry assay, performed at LabCorp or at the University Hospital Cologne.

Measurement of 10-1074 serum levels by TZM.bl. Blood samples were collected immediately before, at the end and 24 h after completion of the 10-1074 infusion, and on days 2, 4, 7, 14, 21, 28, 42, 56, 84, 112, 140 and 168. Levels of active 10-1074 were determined by a TZM.bl neutralization assay[34,40–42]. Serum samples were heat-inactivated for 1 h at 56 °C and measured for neutralizing activity against an HIV-1 strain that was highly sensitive to 10-1074 but resistant to autologous HIV-1 neutralizing serum activity. For individuals without HIV-1 infection, serum samples were tested against Du422 (clade C, tier 2) and ID_{50} values were derived using five-parameter curve fitting. The serum concentration of active 10-1074 was calculated by taking into account the sera ID_{50} titers multiplied by the IC_{50} of 10-1074 for Du422 determined in parallel. In individuals with HIV-1 infection, pre-infusion samples were first tested against a panel of 10-1074-sensitive HIV-1 strains. All individuals showed no or only minimal background activity to 3103.v3.C10 (clade ACD, tier 2), so this strain was used in this study group. ID_{50} values were used to determine 10-1074 serum concentration in the same way as described above. Murine leukemia virus (MuLV)-pseudotyped viruses were used to detect unspecific serum activity and serum samples displaying unspecific activity were excluded from analyses (**Supplementary Table 3**). Serum samples from individuals on ART were tested for neutralizing activity against pseudoviruses produced using an ART-resistant backbone. Briefly, mutations associated with resistance to integrase inhibitors and nonnucleoside reverse transcriptase inhibitors (Q148H, and K101P and Y181C, respectively) were co-introduced into the SG3ΔEnv vector using site-directed mutagenesis. This triple-mutant backbone vector was found to substantially reduce or eliminate ART-associated inhibition against a MuLV control when tested against a large panel of serum samples obtained from individuals on a variety of ART regimens (M.S.S., unpublished data). Testing of serum samples from study participants on ART included an MuLV-pseudotyped triple-mutant virus to detect any residual ART-associated inhibition in the assay.

Pharmacokinetic analysis. Pharmacokinetic parameters were estimated by performing a noncompartmental analysis (NCA) using WinNonlin 6.3.

Virus cultures from individuals with HIV-1. Autologous virus was grown from PBMCs of 179 individuals with HIV-1 under a separate IRB-approved protocol, as previously described[34,37]. Individuals from whom virus was isolated were recruited in New York, USA, and Cologne, Germany, which suggests that the majority are infected with clade B viruses. Culture supernatants were tested for neutralization by 10-1074 as previously described[34,40–42].

Statistical analyses. Pseudovirus neutralization data of 10-1074 was downloaded from the CATNAP database[39] (**Supplementary Fig. 1**). A virus was considered to be neutralized by 10-1074 if the antibody reached an 80% inhibitory concentration (IC_{80}) for a given virus within the range of up to 20 μg/ml. Any virus for which 10-1074 did not reach an IC_{80} within this concentration was considered

not neutralized. Differences in serum half-life of 10-1074 between individuals with and without HIV-1 (**Fig. 1**) were compared by an unpaired two-tailed Student's *t* test with equal variances using GraphPad Prism. The sample size for detecting >0.6 $\log_{10}$ decline in viremia with 80% power at a significance level α of 0.05 was determined to be ten individuals with HIV-1 infection, not on ART, infected with 10-1074-sensitive viruses and assuming that the s.d. would be similar to 10-1074 effects in humanized mice[27]. Curves illustrating average change in viremia after 10-1074 infusions were fitted by robust lowess regression with 40% of the data using MATLAB_R2016a (**Fig. 2a**). The significance of the effect of 10-1074 on viral load was assessed by computing simultaneous confidence bands, and noting when the simultaneous confidence band did exclude a viral load difference of zero (**Supplementary Fig. 5**). Simultaneous confidence bands were computed with the R package locfit (version 1.5-9.1) for each patient subgroup using the Gaussian family for the local likelihood function (**Supplementary Fig. 5**). Nonparametric Spearman coefficients were calculated to assess the correlation between maximum drop in viremia after 10-1074 infusion and baseline sensitivity of autologous viruses to 10-1074 or baseline HIV-1 viral load (**Fig. 2c,d**). CD4+ and CD8+ T cell counts before and after 10-1074 infusion were compared, respectively, by repeated measures one-way ANOVA and *post hoc* Dunnett's multiple comparisons test using GraphPad Prism (**Supplementary Fig. 6**). The neutralization potency of different antibodies against patient-derived pseudoviruses (10-1074 versus PGT121; 3BNC117 versus VRC01) was compared by using a model built on generalized estimating equations (**Fig. 3e**)[57]. Comparisons were drawn on the basis of all day-0 pseudoviruses (*n* = 55). The model was built with intercept and bNAb group as the only covariate. Measurements within a cluster (patient) were assumed to be equi-correlated, and normal distribution was used. *P* values were estimated for the null hypothesis that the weight parameter of the group covariate is zero. GEEQBOX version 1.0 was used for calculations[57].

Single-genome sequencing (SGS) of viral *env* genes. Single-genome amplification and sequencing of HIV-1 *env* genes was performed as described previously[37,58]. Sequences containing premature stop codons or large internal deletions that would compromise *env* functionality were excluded from downstream analyses. Sequences were aligned using CLUSTALW version 2 (ref. 59) and regions that could not be unambiguously aligned were removed from subsequent phylogenetic relationships. Phylograms were constructed using PhyML version 3.1 (ref. 60) using evolutionary models favored by AICc with jModelTest version 2.1.4 (ref. 61) or, for the large data set in **Figure 3a**, RAxML using a GTRGAMMA model[62]. To delineate 10-1074 escape mutations, SGS was performed on day-0 and week-4 plasma samples of 13/14 viremic individuals who responded to the antibody. Plasma samples from nonresponders 1HD2 and 1HD9K were sequenced on day 0 to determine resistance mutations. Week-1 sequencing was performed only on samples with higher viral loads for which sufficient plasma was available. Follow-up sequencing (week 12, week 16, week 20 and week 24) was performed on samples from individuals who remained off ART for more than 12 weeks post-infusion and for which sufficient plasma material was available.

Pseudovirus neutralization assays. CMV promoter-based pseudoviruses were generated as previously described[63]. Pseudovirus supernatants were tested for neutralization by 10-1074, PGT121, 3BNC117, VRC01 and PGDM1400 in a TZM.bl assay as previously described[34,40–42]. Neutralization testing was performed up to 50 μg/ml.

Primer-ID-based deep sequencing of the V3 loop. A Primer-ID deep-sequencing protocol of a ~500-bp region encompassing the base of the V3 loop (HxB2 positions 6,854–7,356) of HIV-1 *env* was designed on the basis of two recently published protocols[49,50]. Five participants were chosen for analysis on the basis of higher viral load and different times of rebound. Primers were designed to bind all five individuals' *env* on the basis of previously obtained SGS sequences. All primers were ordered from Integrated DNA Technologies by using standard desalting as purification, and the cDNA-primer was ordered using hand-mixing of all ten random nucleotides. RNA was extracted from plasma using the Qiagen MinElute Virus Spin Kit. cDNA synthesis was performed using Superscript III and primer 5′-GTGACTGGAGTTCAGACGTGTGCTCTTCCGATCTNNNNN

NNNNNNCAGTTTTACAGTAGAAAAATTCCCCTCCACA-3′. cDNA was purified using Agencourt SPRIselect beads with a bead to reaction ratio of 0.6. All purified cDNA was amplified using primers V3-Forward 5′-GCCTCCCTC GCGCCATCAGAGATGTGTATAAGAGACAGNNNNTGAGCCAATTCCCA TACATTATTGTGC-3′ and ADPT_2a 5′-GTGACTGGAGTTCAGACGTGTG CTC-3′. PCR was performed using Phusion Polymerase and a cycling protocol of initial denaturation at 98 °C for 30 s, 25 cycles of 98 °C for 10 s and 72 °C for 1 min, and then a final extension at 72 °C for 5 min. First-round PCR products were again purified using Agencourt SPRIselect and eluted in a 50-μl volume. 2 μl of the first-round PCR product was then used in a second PCR using primers Universal Adaptor 5′-AATGATACGGCGACCACCGAGATCTACACGCCTC CCTCGCGCCATCAGAGATGTG-3′ and indexed adaptor 5′-CAAGCAGAAG ACGGCATACGAGATNNNNNNGTGACTGGAGTTCAGACGTGTGCTC-3′ that carried a six-nucleotide fixed barcode that allowed for the identification of specific samples. Second-round PCR was performed by using KAPA HiFi Polymerase 2× Ready Mix and cycling conditions of initial denaturation at 95 °C for 2 min, followed by 25 cycles of 98 °C for 20 s, 63 °C for 15 s, 72 °C for 30 s and a final elongation of 3 min at 72 °C. Second-round PCR products were again purified with Agencourt SPRIselect beads, visualized on a 2% agarose gel and gel purified using the Machery-Nagel Gel and PCR Purification Kit. Final products were analyzed by using an Agilent Tapestation and Qubit fluorophotomer. Final products were multiplexed and sequenced paired-end on Illumina MiSeq using 2× 300-bp v3 chemistry. Reads were trimmed using trimfq from seqtk toolkit with an error rate threshold of 1% (-q 0.01) and sequences shorter than 200 nt were removed. Primer IDs were defined as the first 10 nt at the 5′ of each read containing the 5′ cDNA primer. SMALT aligner (v. 0.76) was used to align the primer sequence with up to three mismatches or one gap. Primer IDs containing ten or more sequences were assembled using MIRA (v. 4.0.2) to yield consensus sequences. Consensus sequences containing ambiguity codes were removed for the final analysis. Cross-contamination between subjects was checked by phylogenetic analysis and cross-contaminants were discarded from the analysis. The limit-of-detection of the Primer-ID protocol was estimated for each sequenced patient separately by using a power calculation, as described previously[64]. MATLAB R2016a was used for power calculations using the sampsizepwr function with the binomial distribution option.

Single-molecule real-time sequencing (SMRT sequencing) on Pacific Biosciences RS II. Three participants were selected for SMRT sequencing analysis on the basis of time of rebound, high viral load and sample availability. Full-length HIV *env* was amplified and sequenced on the Pacific Biosciences RS-II, as described previously, with two minor modifications[51]. First, primers were designed specifically for sequenced participants using available SGS sequences that spanned the primer regions. Primers used for amplification were 5′-GAGCAGARGACAGTGGCAATGA-3′ and 5′-GGAGAATAGCTCT ACGAGCTCTTTG-3′ for 1HB3, 5′-GAGCAGAAGACAGTGGCAATGA-3′ (ref. 51) and 5′-TGACCATTTATTGCCCATCTTATAGC-3′ for 1HC2, and 5′-GAGCAGAAGACAGTGGCAATGA-3′ (ref. 51) and 5′-CCACTTGCC ACCCATTTTATAGGA-3′ for 1HD1. Second, the more recent PacBio P6-C4 chemistry was used. Data was preprocessed using the PacBio CCS2 algorithm, generating single-molecule circular consensus sequences. The Full-Length Envelope Analysis (FLEA) pipeline[51] was used for further processing and visualization. MAFFT[65] with manual curation was used to align AA sequences, and fastree2 (ref. 66) was used to infer maximum likelihood phylogenies.

Data availability. HIV-1 envelope SGS data can be downloaded from GenBank (accession numbers KY323724–KY324834). Raw data of Primer-ID sequencing and Pacific Biosciences SMRT have been deposited at the NCBI Short Read Archive BioProject accession number PRJNA356756.

56. Simek, M.D. *et al*. Human immunodeficiency virus type 1 elite neutralizers: individuals with broad and potent neutralizing activity identified by using a high-throughput neutralization assay together with an analytical selection algorithm. *J. Virol.* **83**, 7337–7348 (2009).
57. Ratcliffe, S.J. & Shults, J. GEEQBOX: A MATLAB toolbox for generalized estimating equations and quasi-least squares. *J. Stat. Softw.* **25**, 1–14 (2008).

58. Salazar-Gonzalez, J.F. *et al.* Deciphering human immunodeficiency virus type 1 transmission and early envelope diversification by single-genome amplification and sequencing. *J. Virol.* **82**, 3952–3970 (2008).
59. Larkin, M.A. *et al.* Clustal W and Clustal X version 2.0. *Bioinformatics* **23**, 2947–2948 (2007).
60. Guindon, S. *et al.* New algorithms and methods to estimate maximum-likelihood phylogenies: assessing the performance of PhyML 3.0. *Syst. Biol.* **59**, 307–321 (2010).
61. Darriba, D., Taboada, G.L., Doallo, R. & Posada, D. jModelTest 2: more models, new heuristics and parallel computing. *Nat. Methods* **9**, 772 (2012).
62. Stamatakis, A. RAxML version 8: a tool for phylogenetic analysis and post-analysis of large phylogenies. *Bioinformatics* **30**, 1312–1313 (2014).
63. Kirchherr, J.L. *et al.* High throughput functional analysis of HIV-1 env genes without cloning. *J. Virol. Methods* **143**, 104–111 (2007).
64. Keele, B.F. *et al.* Identification and characterization of transmitted and early founder virus envelopes in primary HIV-1 infection. *Proc. Natl. Acad. Sci. USA* **105**, 7552–7557 (2008).
65. Katoh, K. & Standley, D.M. MAFFT multiple sequence alignment software version 7: improvements in performance and usability. *Mol. Biol. Evol.* **30**, 772–780 (2013).
66. Price, M.N., Dehal, P.S. & Arkin, A.P. FastTree 2—approximately maximum-likelihood trees for large alignments. *PLoS One* **5**, e9490 (2010).